

10th IMC
10th International Masonry Conference
G. Milani, A. Taliercio and S. Garrity (eds.)
Milan, Italy, July 9-11, 2018

FROM POINT CLOUDS TO GEOMETRY GENERATION FOR THE DETAILED MICRO-MODELLING OF MASONRY STRUCTURES

N. Kassotakis¹, V. Sarhosis², J. Mills³, A. D'Altri⁴, S. de Miranda⁵, G. Castellazzi⁶

¹ PhD student, School of Civil Engineering and Geosciences, Newcastle University
School of Engineering, Newcastle University, Newcastle upon Tyne, UK,
e-mail: n.kassotakis2@newcastle.ac.uk

² Assistant Professor, School of Engineering, Newcastle University
School of Engineering, Newcastle University, Newcastle upon Tyne, UK,
e-mail: vasilis.sarhosis@newcastle.ac.uk

³ Professor, School of Engineering, Newcastle University
School of Engineering, Newcastle University, Newcastle upon Tyne, UK,
e-mail: jon.mills@newcastle.ac.uk

⁴ PhD student, Department of Civil, Chemical, Environmental, and Materials Engineering (DICAM), University of Bologna, Bologna, Italy,
e-mail: antoniomaria.daltri2@unibo.it

⁵ Professor, Department of Civil, Chemical, Environmental, and Materials Engineering (DICAM), University of Bologna, Bologna, Italy,
e-mail: stefano.demiranda@unibo.it

⁶ Assistant Professor, Department of Civil, Chemical, Environmental, and Materials Engineering (DICAM), University of Bologna, Bologna, Italy,
e-mail: giovani.castellazzi@unibo.it

Keywords: Point cloud, numerical modelling, geometry, micro-modelling, DEM.

Abstract. *Over the last few decades a significant effort has been put on the development of detailed numerical models to predict the mechanical behavior of historical masonry. However, an issue faced in the numerical modelling of historic and damaged masonry structures is the development of accurate models to represent their real geometries. This paper presents the first stage of a research program which aims to develop an automatic approach which uses point clouds to generate the detailed geometry of masonry. Such geometry can then be inputted into micro-models for the structural analysis of masonry structures. In the proposed approach, point clouds generated using the Structure-from-Motion (SfM) pipeline were converted into watertight meshes and then voxelized. Models were represented as a sum of cuboid-blocks jointed by zero thickness interfaces. The developed methodology was applied to derive geometries of two small scale masonry specimens constructed in the laboratory and a full-scale masonry arch bridge.*

1 INTRODUCTION

Over the last three decades, a significant effort has been put on the development of accurate structural analysis models to represent the complex and highly nonlinear mechanical behavior of masonry [1, 2]. Such models range from considering masonry as an anisotropic continuum (e.g. macro-models based on the finite element method) to the more detailed ones considering masonry as an assemblage of units and mortar joints (e.g. micro-models based on the discrete element method [3]).

Recent research [4, 5, 6, 7] demonstrated that when modelling masonry using the micro-modelling approach, the accuracy of the model's results is directly related to: a) the global geometrical characteristics of the structure (e.g. dimensions of the boundary of the structure); and b) the detailed (or local) geometrical characteristics (e.g. actual shape, location and orientation of masonry units and mortar joints in the structure etc.). Today, the commonplace procedure of obtaining the geometry of a masonry structure is using traditional surveying techniques (e.g. leveling and total stations. However, this can be both time and resource consuming and often inaccurate, especially when one wants to obtain the location of individual masonry units in a structure. Therefore, over the last few years, there has been an extensive interest to develop approaches to obtain accurate geometries of complex masonry structures from point clouds and automatically input them into advanced numerical software for their structural analysis.

Truong and Laefer [8] developed a FEM model from point clouds obtained via terrestrial laser scanning to investigate the impact of window shape, brick orientation, window size, and the presence of lintels. Truong-Hong et al. [9] modelled façades using FEM software utilizing laser scans for input. Through a FacadeAngle (FA) algorithm, it was proposed to create boundaries of façade features through the combination of an angle criterion and voxelization. Later, Truong and Laefer [10] approached the same problem again but with the inclusion of an octree representation. In addition, Zolanvari and Laefer [11] introduced the "*Slicing Method*" on overall method of extracting façade and window boundary points for reconstructing a façade into a geometry compatible with computational modelling. After finding a principal plane, the façade was sliced into limited portions with each slice representing a unique, imaginary section passing through a building. Finally, on modelling historical buildings, Castellazzi et al. [12] applied a slicing algorithm to point cloud data obtained from laser scanning and produced a voxelized mesh from joining each sliced segment. This was subsequently converted into a solid model that was used for the structural analysis of historic masonry structures using the FEM.

Furthermore, a few studies used point clouds to develop the geometry of masonry arch bridges and carry out structural analysis. Armesto et al. [13] presented the application of laser scanning and ground penetrating radar (GPR) to develop a FEM model of a masonry arch bridge. The modelling procedure consisted of cleaning and segmenting the point cloud, applying 2D Delaunay triangulation to the point cloud surface and adding texture to these surfaces with contemporaneous photographs. The product of FEM modelling was a sensitivity analysis of the Young moduli of the bridge. Also, Arias et al. [14] presented a point cloud processing method for estimating deformations in masonry arch bridges. The arch geometry was obtained by means of a laser scan survey and the resulting point cloud was processed by statistical non-parametric methods based on local bivariate kernel smoothers. Riveiro et al. [15] created a simplified method of modelling masonry arch bridges from the combination of laser scanned point clouds and orthoimagery. Structural assessment was performed using analysis based on the limit-state assessment. The basic workflow utilized in this study was: (a) application of 2D Delaunay triangulation and addition of texture to the surfaces using photographs; (b) extraction of the final geometrical models in CAD; (c) calculation of the safety factors for the bridges via the thrust-line calculation in Matlab utilizing the CAD model orthoimagery. Gonzalez et al. [16] described

the development of a point cloud processing methodology focused on recognizing the degradation of mortar in masonry arch bridges by means of efflorescence detection. Puente et al. [17] demonstrated an application of point cloud processing to evaluate and record damage in masonry arch bridges by cloud to cloud comparison. The method consisted of combining 3D point clouds and orthoimages to create a 3D CAD model. Although no further structural assessment followed, pathologies were considered by comparing the 3D model with an assumed undeformed. Riveiro et al. [18] created a generalized semi-automated methodology of segmenting point clouds and generating geometries of masonry arch bridges. In addition, Riveiro et al. [19] performed an inverse analysis on a failed bridge using Discrete Finite Element Method (DFEM) modelling. The initial undamaged geometry was assumed and the deformed created through an automatic point cloud processing procedure. In specific, the bridge's main features such as the face were extracted by plane fitting. Further details of masonry joint locations were retrieved by utilizing the intensity images of the TLS data. The inverse analysis was produced by comparing displacements of the deformed with the assumed undamaged model. This was via global optimization approach by means of a genetic algorithm. Finally, Conde et al. [20] applied a multidisciplinary approach to structurally assessing a MAB including TLS, ground penetrating radar, sonic testing and modal identification tests. The geometry was semi-automatically extracted and assessment was carried out with FEM software.

Although semi-automated and automated procedures which use point clouds to generate geometries for the structural analysis of full scale masonry structures using the macro-modelling approach exist (e.g. homogeneous finite element models, discrete finite element models), to date there has been no reported work in automated procedures for modelling full scale masonry structures using the detailed micro-modelling approach with fully discrete element models.

The aim of this paper is to present the development of a semi-automated approach for generating the detailed geometry of a masonry structures which can later be inputted in micro-models (such as the commercial software package 3DEC [21]) for their structural analysis.

The layout of this paper is as follows: Section 2 provides a description of the applied photogrammetric, mesh and numerical modelling methodology. Section 3 reports the results of the application of the methodology on two small-scale experimental structures and preliminary application to a full-scale masonry arch bridge. Section 4 presents the main conclusions of the work achieved to date.

2 METHODOLOGY

There are three main methods for developing structural models directly from point cloud data. These are: a) constructive solid geometry (CSG); b) boundary representations (B-reps); and c) spatial subdivision representations [22]. In the first method, objects are represented using Boolean combinations of simpler objects. For the second method, object surfaces are represented either explicitly or implicitly. For the third method, an object domain is decomposed into cells with simple topologic and geometric structure, such as regular grids and octrees. The developed procedure of this paper pertains to the third group of spatial subdivision representation. The creation of the final model consisted of four major steps: a) capturing the point cloud; b) mesh construction; c) mesh voxelization; d) solid model development from the voxelized mesh. These steps will be discussed in further detail below.

2.1 Workflow

Figure 1 presents the workflow of the semi-automated approach for processing point clouds. The first step refers to the process of obtaining the point cloud. Point clouds can be obtained

either by laser scanning and/or photogrammetry. The second step deals with the mesh generation. The point cloud needs to be cleaned and segmented. Then, the mesh must be repaired/cleaned and made watertight. The third steps comprise mesh voxelization and converting the final voxelized mesh into a solid model. The end result is readable geometry file for input into the discrete element software (e.g. in this case 3DEC).

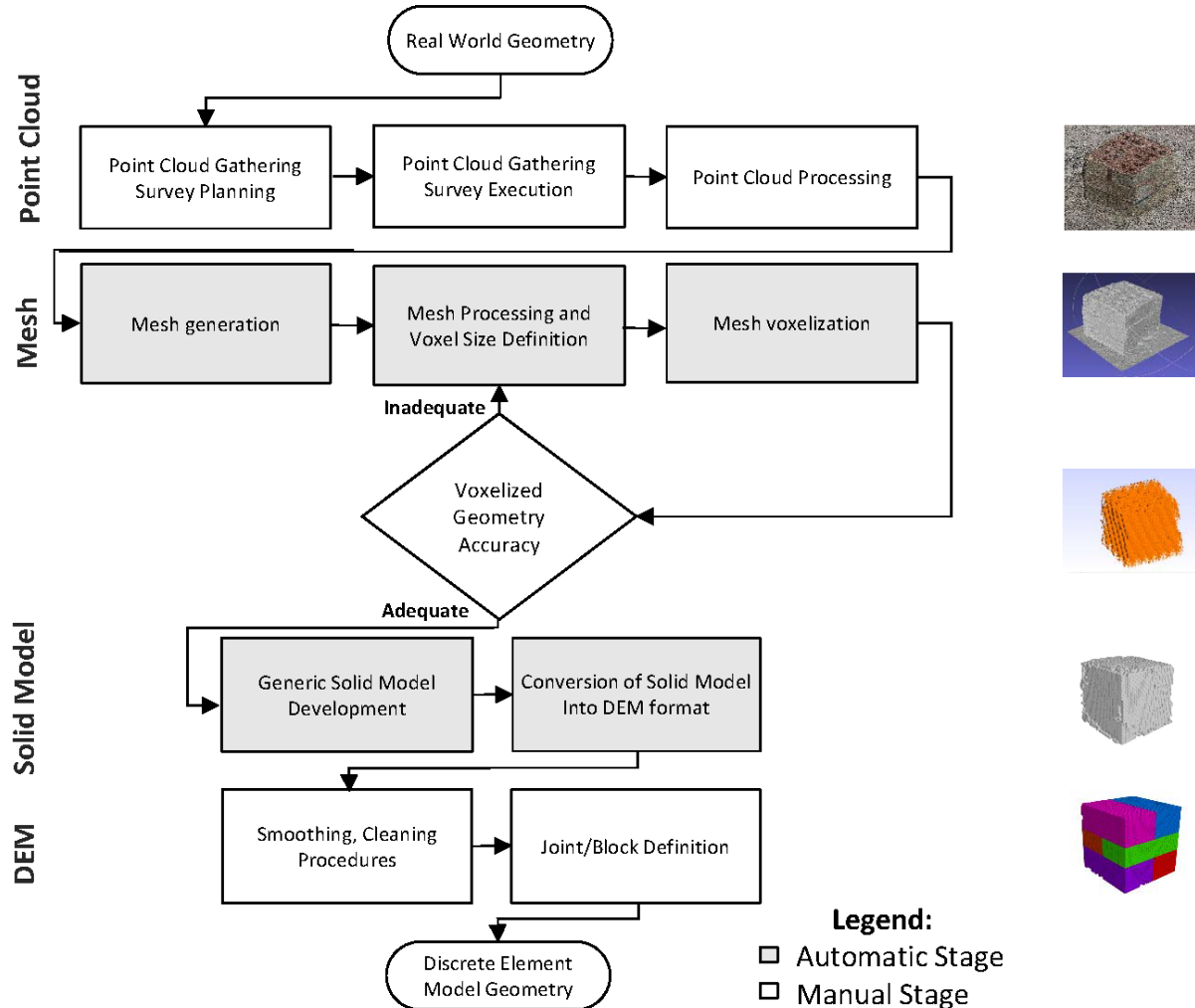


Figure 1: Workflow of the developed semi-automated approach.

The aforementioned survey techniques generate dense clouds of 3D points. For full-scale historical structures, such as the fortress of San Felice sul Panaro (Italy), a point cloud density range of 10,000 to 40,000 pts/m² has been shown to lead good rapport between dataset manageability and accuracy of geometry representation [12]. Finally, after obtaining the dense point cloud, points not relevant to the structure must be removed. This is done mainly by removing all irrelevant neighbouring points from point cloud.

A Poisson surface reconstruction was used to create a watertight mesh. The Poisson surface reconstruction algorithm produces surfaces corresponding to solutions of the Poisson equation and is an established computer graphics technique for creating watertight surfaces from point samples. The resulting surfaces are very smooth without noisy data [12]. All utilised operations are standardized and may be conducted by most 3D mesh processing software packages.

The resulting solid model is created by subdividing the watertight mesh's volume into a sum of voxels. This procedure is termed voxelization and is implemented using well-established

algorithms. The selected voxel dimension is chosen relative to the structure's size. A good range has been previously identified between 0.05 and 0.25 m for typical historic structures [12]. The final voxel model is a three-dimensional matrix that contains values relative to the voxels spatial location and consistency (void or active). Thus, the DEM model is developed in the form of 8-node hexahedral Discrete Elements in a procedure commonly applied in a FEM background [12]. Figure 2 shows the notion of the voxelized solid model and its voxel elements in an x-y-z coordinate system. In Figure 2, the numbers denote nodes of the voxelized mesh, the grey zone depicts a single voxel and the quantities Δx , Δy and Δz the size of the voxel's vertices.

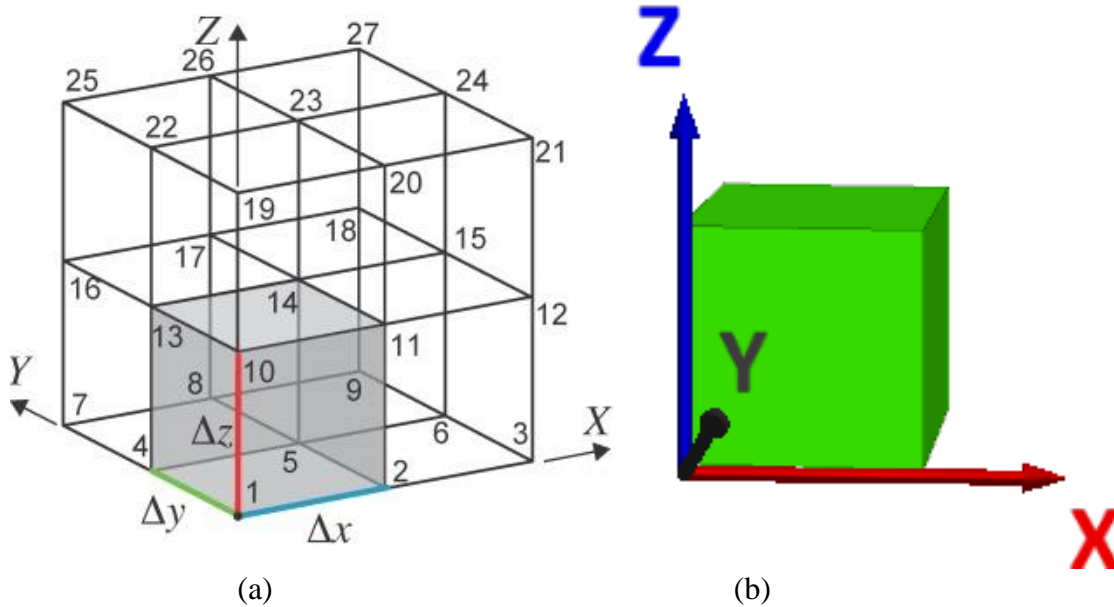


Figure 2: The notion of voxels inside: (a) the Solid Model [12]; and (b) the DEM model.

3 EXPERIMENTAL PROOCEDURE

3.1 Experimental setup

Using two simple masonry specimens constructed in the laboratory, synthetic data generated in order to assess the feasibility of the proposed approach. The masonry specimens constructed in the laboratory are shown in Figure 3. These were purposely built to cover the cases of orthogonal and curved structures. The first structure was a brick stack prism made of six regular size building bricks which were joined without mortar. Due to irregularities in the masonry units, the joint between the blocks was not zero. However, for simplifications, in this study, it was assumed as zero. The second specimen involved a small scale arch made of 22 experimental block elements with a zero mortar thickness. The equipment used for data collection was a DSLR camera and a tripod. Finally, the lighting of the space was artificial. The geometrical details of the experiment are shown below in Table 1.

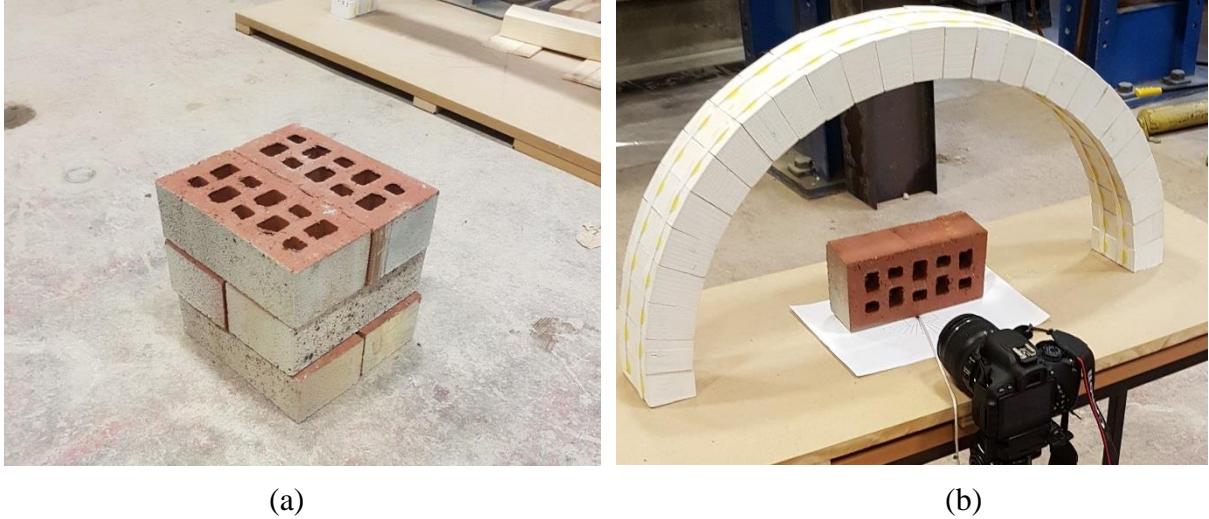


Figure 3: Experimental setup: (a) Brick prism; and (b) Experimental Arch.

Experiment	Length [mm]	Width [mm]	Height [mm]	Block Number	Mortar Thickness
Brick Prism	210	210	190	6	0
Exp. Arch	670	100	335	27	0

Table 1: Dimensions of the specimens tested in the laboratory.

3.2 Point cloud collection and handling

The first stage of any photogrammetric survey is that of network planning which depends on the object to be surveyed. Photographs were taken from a radial distance of 1 m from the geometrical centroid of the ground plan for each of the two objects. Photography was taken from two levels. For the brick-prism, a single height of 1 m was needed. For the arch two heights of photography were used: 0 m and 0.75 m relative to the arch’s base level. Overlapping imagery was acquired to ensure a fully detailed model. Photographs were taken in a circular motion around the objects with a 10 degree angle between each frame. Finally, an overlap of at least 50 percent was ensured between consecutive images. Figure 4 shows the ground plan of the photogrammetric survey. Figure 5 shows the point clouds gathered via photogrammetric survey for a full circle of 360 degrees.

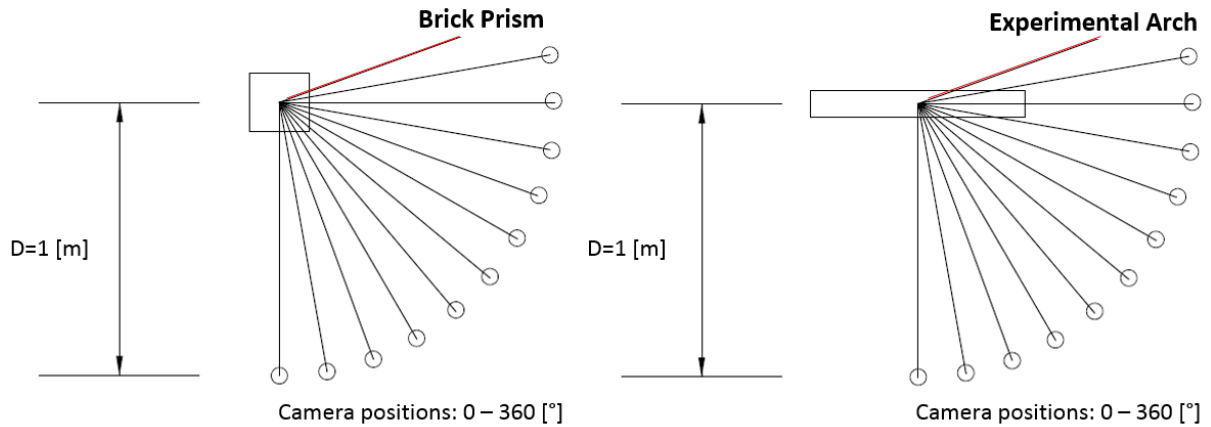


Figure 4: Plan of the photogrammetric survey network.



Figure 5: Dense Point Clouds of (.ply format): (a) Brick Prism; and (b) Experimental Arch.

3.3 Mesh preparation and processing

3.3.1 Mesh preparation

The mesh handling and processing was undertaken using the program MeshLab [23]. A cleaning procedure was initially imposed to remove redundant vertices from the mesh. A surface screened Poisson surface reconstruction was then used to make the mesh watertight, a prerequisite for voxelization. Figure 6 shows the final watertight meshes.

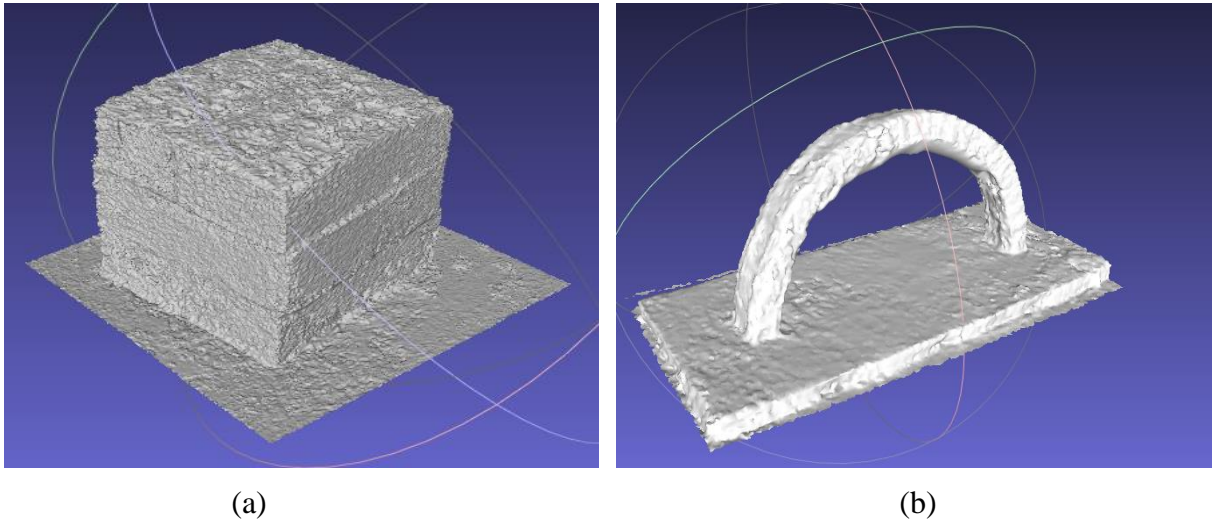


Figure 6: Mesh preparing and processing: (a) Brick Prism; and (b) Masonry Arch.

3.3.2 Mesh voxelization

Mesh voxelization was executed in the program Bivox [24]. This is an open-source program initially developed for the needs of geometry development for computer gaming. This part was essential, because the surface based triangles of a typical triangulated mesh (e.g. Delaunay triangulation) are hard to handle in the DEM software, leading to unstable numerical solutions. In essence, this stage means defining the enclosed volume of the watertight mesh as a sum of cuboids (voxels). This is especially useful because the voxel dataset means each voxel can be

directly transformed into an 8-noded discrete element. The voxel size is user defined and trials were executed to determine the optimum size. Figure 7 shows the final selected sizes the actual data size of the models compared to their voxel size. Smaller voxel sizes (e.g. Figure 7 (b)) gave a more accurate geometric representation but were much more computationally demanding.

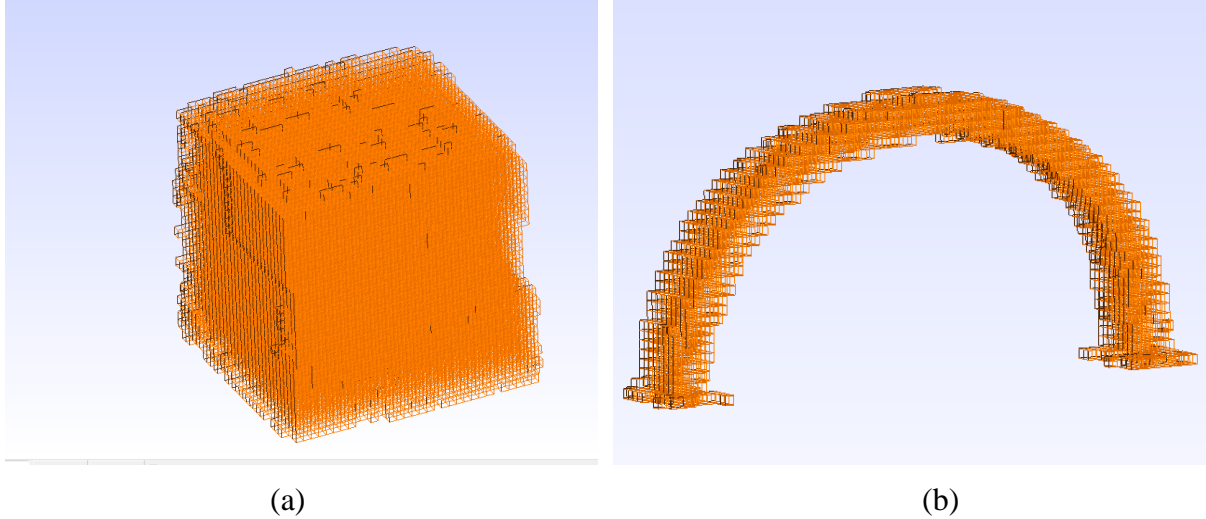


Figure 7: Mesh Voxelization (.msh file format): (a) Brick masonry prism (0.8 mm^3 voxels), (b) Masonry Arch (2 mm^3 voxels).

Model	Voxel Size [mm]	Voxel Number	DEM Model Size MB]
Brick Prism	0.8	30215	18.75
Exp. Arch	2	16692	6.173

Table 2: Dimensions and Characteristics of the Voxelized Meshes

3.4 Solid model

The voxelized meshes were converted into an input file using the program Gmesh [25]. As there was not an option to automatically output models directly into the DEM's program format, the models were exported into FEM Abaqus [26] (.inp) format files which had a similar file structure to that of the DEM software package 3DEC. In this way, each 8-noded finite element voxel was converted into a discrete element and in particular a polyhedron. Thus, each voxel of the previous voxelized mesh became a cuboidal polyhedron in the DEM software. The procedure of converting the finite elements of the .inp file to corresponding polyhedrons in the 3DEC geometry file was completed in Microsoft Excel.

3.5 Discrete Element Model

3.5.1 Model development, preprocessing and smoothing

The DEM code provided the ability to develop multiple block elements which were defined by two assumptions: a) an unlimited permissible amount of vertices; and b) the two faces of the prism were to be parallel. In this way, the nodes and elements were transformed into corresponding 8-nodes polyhedrons of the DEM software, displayed below in images of Figure 9(a) and Figure 9(b). However, these models contained some irregularities upon their surfaces in the

form of neighboring voxels. This was due to the fact that the face of the mesh, prior to voxelization was not entirely planar leading to the representation of the non-planar space by voxels too. To overcome this, a smoothing procedure was induced into the DEM code, in the form of simply deleting the blocks outside the boundary of the modelled objects. Limitations were existent in this smoothing process for the case of the curved surface of arch. In this case the proposed solution, was to define a smaller voxel size as to approximate the curved surface.

3.5.2 Model joint and block definition

For the brick-prism's final geometrical representation, it was aimed to define each of its bricks as discrete element. There were two methods detected to segment the brick-prism model inside the code itself. The first was by means of joining voxels of a certain region to constitute a brick. The second was via joining all the blocks of the model and subdividing it into bricks via a splitting routine. Comparing the both methods, the latter was preferred because contrarily with the joining method, joints could be imposed wherever needed with the splitting method. The below images of figure 9(c) and 9(d) depict the application of both segmenting procedures, before and after the (splitting). The splitting was imposed for the vertical joints. The horizontal joints were a result of joining blocks within a given block height range and thus coincide with actual voxel boundaries. Finally, the models were joined and split (figure 10) with the given coordinates, and orientation of the actual blocks in simplistic way. For the experimental arch's final geometrical representation, the goal was to segment the arch into actual voussoirs. Due to its curvature, only the splitting technique was deemed applicable. It was applied by radially splitting the arch into segments.

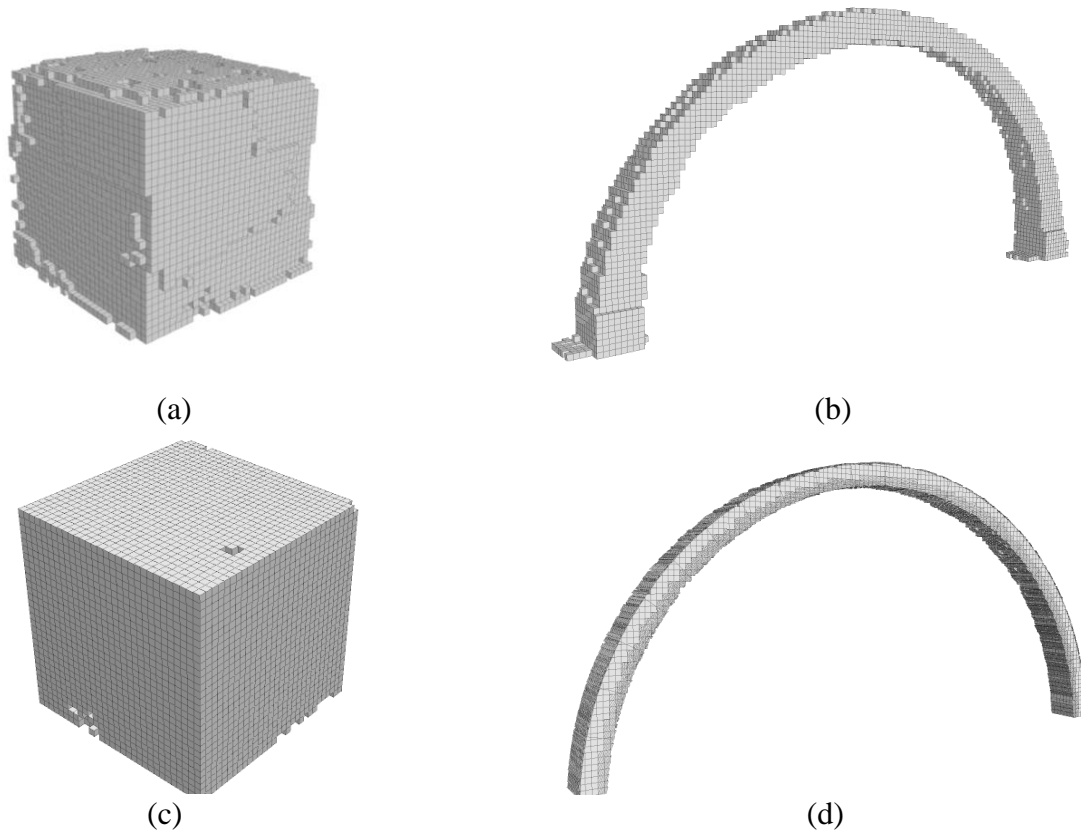


Figure 9: DEM Models: (a) Brick prism, initial; (b) Experimental Arch, initial; (c) Brick prism, smoothed; and (d) Experimental Arch, smoothed.

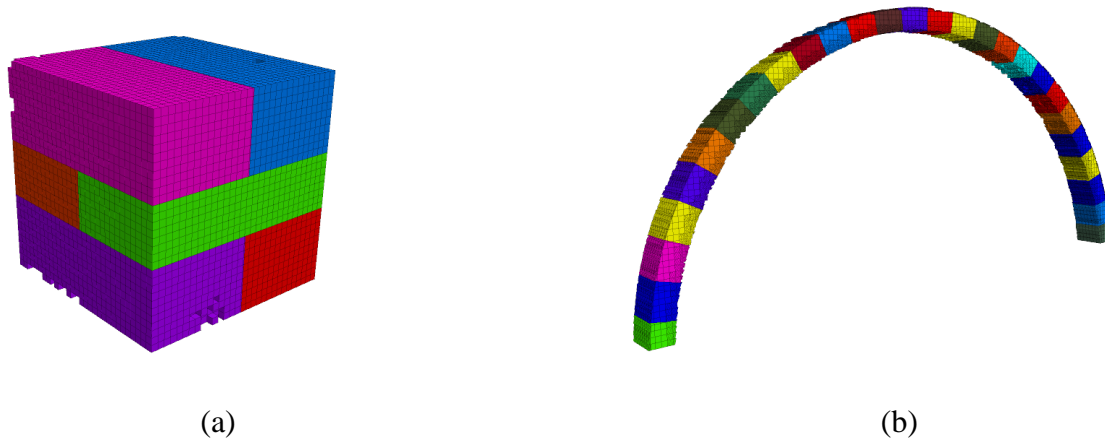


Figure 10: DEM Models after smoothing and with joints: (a) Brick prism; and (b) Experimental Arch.

3.6 Application on a full-scale masonry arch bridge

The proposed procedure applied to Lambton Bridge, which is a Grade 2 listed, masonry arch bridge located on the Lambton Estate, Chester-le-Street, England. The bridge, depicted in figure 11, was designed by Ignatius Bonomi and spans the River Wear. It was originally a 25 m span. However, due to subsidence and converging abutments, the bridge now spans 24.85 m. Its point cloud was procured from part of an existing survey and in specific, a laser scan from all four diagonal extremities with sequential registration.



Figure 11: Lambton Bridge: (a) Original shape; and (b) Current deformed shape.

The procedure of modelling the geometry of the bridge was identical to that undertaken for the small-scale samples. After the point cloud was acquired (Figure 12a.), processed and cleaned it was converted into a watertight mesh. It must be noted that some simplifications were made. For instance, some parts of the bridge which do not participate in the load-bearing were removed from the initial point cloud and consequently mesh. As the main variable parameter of the whole modelling is the voxel size, various voxel sizes were used to assess their adequacy and model efficiency.

The final voxel size was 30 cm and selected based on satisfying on three factors: a) that the model's surface smoothness be acceptable or accepting to smoothing inside the code; b) that

the curvature of both the arch (x-z plane) and spandrel walls (x-y plane) to be adequately approximated by the voxels; and c) that the total model size be within a range of realistic computational resources. Thus, the resulting initial DEM model had 53722 elements in size. Figure 12 shows the application of all the workflow on the bridge.

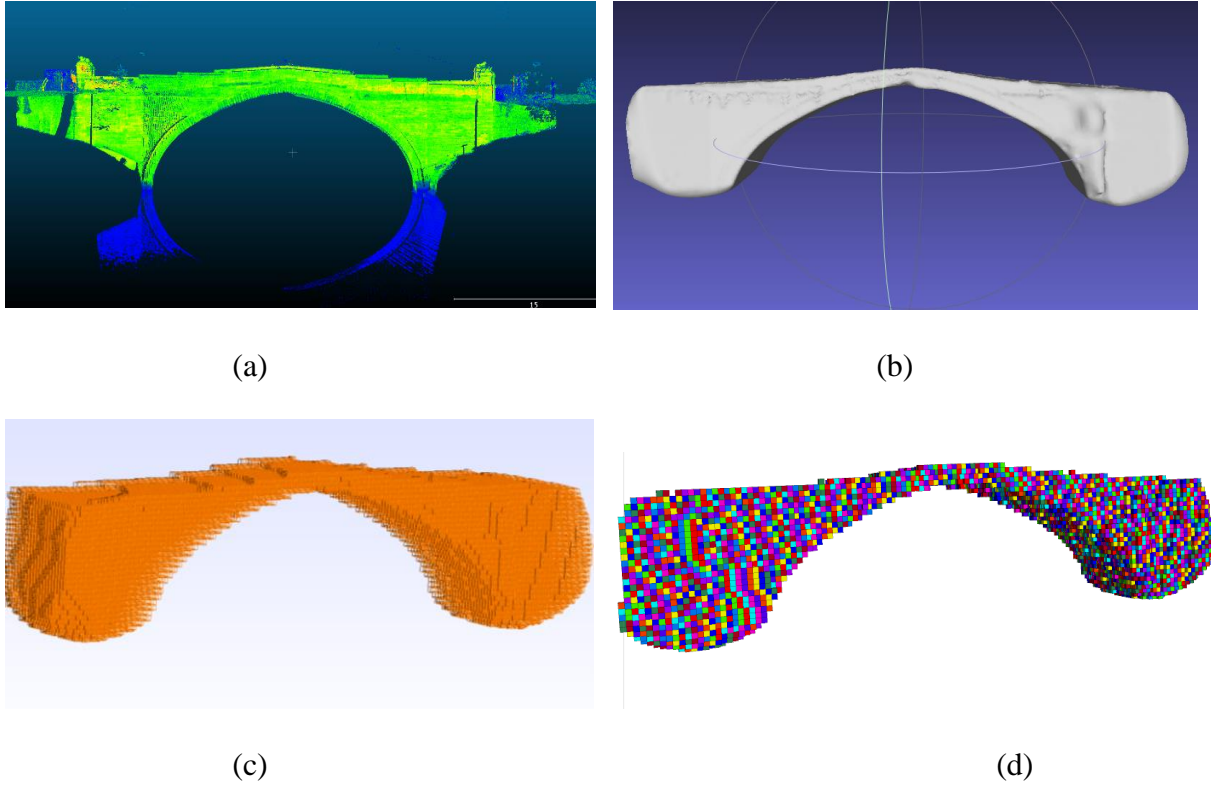


Figure 12: Lampton Bridge: (a) Mesh, (b) Voxels (30 cm^3 voxels) Point Cloud, (c) Voxelized Mesh, (d) Initial DEM model.

The initial DEM model was furthermore smoothed and segmented inside the DEM code in the same manner as the experimental models. Figure 13 shows the model of the bridge after it was smoothed and segmented into its main constitutive members including: a) the arch ring (multi-colored voussoir elements); b) the spandrel walls (green); and c) the arch fill (red). Finally, a simplified assumption of block/joint definition was applied for each section. The arch ring was subdivided into voussoirs with a length equal to the depth of the bridge. For the spandrel walls and fill, each voxel was considered a block.

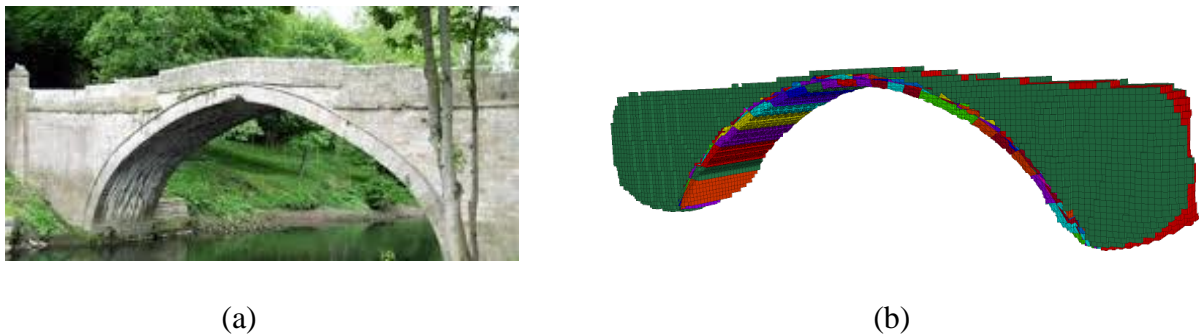


Figure 13: Lampton Bridge: (a) current deformed state; and (b) final Model.

4 CONCLUSIONS

This paper presented a semi-automatic approach which uses point clouds to generate the detailed geometry to be used for the structural analysis of masonry structures. Initially, coarse models were generated from point clouds. Subsequently the models were smoothed and segmented. The developed approach was applied on small-scale orthogonal and curved structures with promising results. A full-size application showed its applicability on a full scale masonry arch bridge. The procedure was found to be cost-effective and easy to implement. However, the method found to have the following two main limitations: a) the models inherent necessity to be manually cleaned and smoothed; and b) the method's dependency on manual definition of the local features of the geometry (blocks, joints). Further studies are required to be carried out in the future to overcome the above limitations.

ACKNOWLEDGEMENTS

The work presented in this paper is financially supported by an EPSRC doctoral training award (case/179/65/82). Further acknowledgement is duly given to Gabriel Lee Stockdale for constructing the experimental arch, the Lampton Estate and Bill Harvey Associates Ltd. for providing mentoring and full access to the case study bridge.

REFERENCES

- [1] P.G. Asteris, V. Sarhosis, A. Mohebbkhah, V. Plevris, L. Papaloizou, P. Komodromos, J.V. Lemos. Numerical modelling of historic masonry structures, *Handbook of Research on Seismic Assessment and Rehabilitation of Historic Structure*, **12**, 213-256, 2015.
- [2] V. Sarhosis, J.V. Lemos, K. Bagi, G. Milani, *Computational modelling of masonry structures using the discrete element method*, IGI Global: USA, 2016.
- [3] V. Sarhosis, J.V. Lemos, K. Bagi, G. Milani, Micro-modelling options for masonry structures, Chapter 2. In: *Computational modelling of masonry structures using the discrete element method*, V. Sarhosis, Vol. 1, IGI Global, 2016.
- [4] V. Sarhosis, P.G. Asteris, T. Wang, W. Hu, Y. Han, On the stability of colonnade structural systems under static and dynamic loading conditions. *Bulletin of Earthquake Engineering*, **14**(4), 1131-1152, 2016.
- [5] V. Sarhosis, S. De Santis, G. de Felice, A review of experimental investigations and assessment methods for masonry arch bridges. *Structure and Infrastructure Engineering. J. Mechanics Research Communications*, **12** 1439-1464, 2015.
- [6] F. Szakály, Z. Hortobágyi, K. Bagi, Discrete Element Analysis of the Shear Resistance of Planar Walls with Different Bond Patterns. *The Open Construction and Building Technology Journal*, **10**, 190-202, 2016.
- [7] T. Forgács, V. Sarhosis, K. Bagi. Minimum thickness of semi-circular skewed masonry arches. *Engineering Structures*, **40**, 317–336, 2017.

- [8] L. Truong-Hong, D. Laefer, Impact of modeling architectural detailing for predicting unreinforced masonry response to subsidence. *Automation in Construction*, **30**, 191–204, 2013.
- [9] L. Truong-Hong, D. Laefer, T. Hinks, H. Carr, Combining an Angle Criterion with Voxelization and the Flying Voxel Method in Reconstructing Building Models from LiDAR Data. *Computer-Aided Civil and Infrastructure Engineering*, **28**, 112–129, 2013.
- [10] L. Truong-Hong, D. Laefer, Octree-based, automatic building façade generation from LiDAR data. *Computer-Aided Design*, **53**, 46–61, 2014.
- [11] I. Zolanvari, D. Laefer, Slicing Method for Curved Façade and Window Extraction from Point Clouds. *ISPRS Journal of Photogrammetry and Remote Sensing*, **119**, 334–346, 2016.
- [12] G. Castellazzi, A. D'Altri, G. Bitelli, I. Selvaggi, A. Lambertini, Alessandro, From Laser Scanning to Finite Element Analysis of Complex Buildings by Using a Semi-Automatic Procedure. *Sensors*, **15**, 18360–18380, 2015.
- [13] J. Armesto, P. Arias, J. Roca, H. Lorenzo, Monitoring and Assessing Structural Damage in Historic Buildings. *The Photogrammetric Record*, **23**, 36–50, 2008.
- [14] P. Arias, B. Riveiro, J. Armesto, S. Carracelas, Mercedes, Terrestrial laser scanning and non-parametric methods in masonry arches inspection. *International Archives of the Photogrammetry, Remote Sensing and Spatial Information Sciences - ISPRS Archives*, **38**, 39–44, 2010.
- [15] B. Riveiro, P. Morer, P. Arias, I. De Arteaga, Terrestrial laser scanning and limit analysis of masonry arch bridges. *Construction and Building Materials*, **25**(4), 1726–1735, 2011.
- [16] H. Gonzalez, I. Puente, B. Riveiro, J. Martínez-Sánchez, P. Arias, Automatic segmentation of road overpasses and detection of mortar efflorescence using mobile LiDAR data. *Optics & Laser Technology*, **54**, 353 – 361, 2013.
- [17] I. Puente, M. Solla Carracelas, H. Gonzalez, P. Arias, NDT documentation and evaluation of the Roman Bridge of Lugo using GPR, mobile and static LiDAR. *Journal of Performance of Constructed Facilities*, **29** (1), 06014004, 2013.
- [18] B. Riveiro, M. Dejong, B. Conde, Automated processing of large point clouds for structural health monitoring of masonry arch bridges. *Automation in Construction*, **72** 258–268, 2016.
- [19] B. Riveiro, B. Conde, G. Drosopoulos, G. Stavroulakis, M. Stavroulaki, Fully automatic approach for the diagnosis of masonry arches from laser scanning data and inverse finite element analysis. *Proc. of the 10th Int. Conf. on Structural Analysis of Historical Constructions*. SAHC, Leuven, Belgium, 133–139, 2016.
- [20] B. Conde, F.L. Ramos, D. Oliveira, B. Riveiro, M. Solla Carracelas, Structural assessment of masonry arch bridges by combination of non-destructive testing techniques and three-dimensional numerical modelling: Application to Vilanova bridge. *Engineering Structures*, **148**, 621–638 2017.
- [21] 3DEC Itasca. 3-Dimensional Distinct Element Code Manual, Itasca Consulting Group, Minneapolis. 2017

- [22] T. Hinks, H. Carr, L. Truong-Hong, D. Laefer, Point Cloud Data Conversion into Solid Models via Point-Based Voxelization. *Journal of Survey Engineering*, **139**(2), 72-83, 2012.
- [23] Meshlab (version 2016.12). Retrieved from www.meshlab.net/, 2018.
- [24] Min P, Binvex (version 2.1). Retrieved from <http://www.patrickmin.com/binvox/>, 2018.
- [25] C. Geuzaine, J.-F. Remacle. Gmsh: a three-dimensional finite element mesh generator with built-in pre- and post-processing facilities. *International Journal for Numerical Methods in Engineering*, **79**(11), 1309-1331, 2009.
- [26] ABAQUS UNIFIED FEA (version 2018). Retrieved from <https://www.3ds.com/products-services/simulia/products/abaqus/>, 2018.